

## Quasi solid state dye-sensitized solar cells based on polyvinyl alcohol (PVA) electrolytes containing $I^-/I_3^-$ redox couple

A. K. Arof · M. Naeem · F. Hameed · W. J. M. J. S. R. Jayasundara · M. A. Careem · L. P. Teo · M. H. Buraidah

Received: 29 April 2013 / Accepted: 17 June 2013 / Published online: 29 June 2013  
© Springer Science+Business Media New York 2013

**Abstract** Quasi solid state dye-sensitized solar cells (DSSCs) have been fabricated with electrolytes containing  $I^-/I_3^-$  redox couple using 80 % hydrolyzed polyvinyl alcohol (PVA) doped with potassium iodide (KI) and a mixture of potassium iodide and tetrapropyl ammonium iodide ( $Pr_4NI$ ) salts. The quasi solid state gel polymer electrolytes were prepared using 1:1 ethylene carbonate (EC):propylene carbonate (PC) mixture. The solar cells have the structure of ITO/TiO<sub>2</sub>/N3-Dye/electrolyte/Pt/ITO. The conductivity of the electrolytes has been calculated from the bulk resistance value determined using the electrochemical impedance spectroscopy. The performance of the DSSCs has been studied by varying the concentration of the doping salts in the electrolyte and incident light intensity. The DSSC fabricated with the KI salt electrolyte containing 9.9 wt% PVA, 39.6 wt% EC, 39.6 wt% PC, 10.9 wt% KI(+I<sub>2</sub>) exhibited the best power conversion efficiency of 1.97 %. However, the DSSC with a double-salt electrolyte containing 9.9 wt% PVA: 39.6 wt% EC: 39.6 wt% PC: (6.5 wt% KI: 4.4 wt%  $Pr_4NI$ ) (+I<sub>2</sub>) exhibited a higher efficiency of 3.27% under 100 mW/cm<sup>2</sup> light intensity. The efficiency of this cell increased to 4.59 % under dimmer light of intensity of 54 mW/cm<sup>2</sup>.

**Keywords** Quasi solid-state dye-sensitized solar cells (DSSCs) · Polyvinyl alcohol (PVA) · Double-salt

---

A. K. Arof (✉) · M. A. Careem · L. P. Teo · M. H. Buraidah  
Department of Physics, Centre for Ionics University of Malaya, University of Malaya,  
50603 Kuala Lumpur, Malaysia  
e-mail: akarof@um.edu.my

M. Naeem  
Department of Chemical and Biological, Chalmers University of Technology, Göteborg, Sweden

F. Hameed  
Department of Applied Physics, Chalmers University of Technology, Göteborg, Sweden

W. J. M. J. S. R. Jayasundara  
Postgraduate Institute of Science, University of Peradeniya, Peradeniya, Sri Lanka

## 1 Introduction

Due to its abundance in the earth's crust, silicon has been the primary element used in the fabrication of semiconductor devices including solar cells. However, the extraction of high quality silicon is complex and expensive and this has contributed to the high cost of silicon solar cell manufacturing. The use of dye-sensitizers in conjunction with other materials have provided an alternative and relatively easier way for manufacturing solar cells with lower production cost (O'Regan and Grätzel 1991; Nazeeruddin et al. 2001). The first dye sensitized solar cell was reported by O'Regan and Grätzel (1991) and since then intensive research on photoelectrochemical dye-sensitized solar cells (DSSCs) are carried out all over the world.

A DSSC consists of an electrolyte that serves to restore the dye after oxidation of its molecules. The electrolyte basically contains a redox mediator in an organic matrix (Nazeeruddin et al. 2001). There have been different types of mediators used in the electrolytes e.g.  $I^-/I_3^-$ ,  $SCN^-/(SCN)_2$ , Co(II/III) and S/S<sup>2-</sup> (Sapp et al. 2002; Oskam et al. 2001). The most commonly used mediator is the  $I^-/I_3^-$  couple because of its slow recombination rate with injected electrons (Oskam et al. 2001; Santa-Nokki et al. 2007; Lan et al. 2008). DSSCs based on liquid electrolytes have exhibited certified efficiencies up to 11.4 % (Chiba et al. 2006) and uncertified efficiencies up to 12.3 % (Jeonga et al. 2011). However, there are problems associated with liquid electrolytes that affect the reliability of the DSSC. For example, liquid electrolytes can evaporate and leak, thus affecting the long-term stability of DSSCs (Grätzel 2003). The use of solid electrolytes such as polymer electrolytes can help overcome these problems. A solid polymer electrolyte is basically a solvation of a salt in a polymer matrix.

A major challenge in the fabrication of DSSCs employing solid polymer electrolyte is good electrolyte/electrode contact. A good interfacial contact is very important for improving the efficiency of the device. A method to overcome the contact problem is to use a gel electrolyte or better known as quasi-solid electrolyte. Gel electrolytes have higher ionic conductivity than solid polymer electrolytes due to the presence of trapped liquids in the polymer matrix. The flexibility of gel electrolytes enables them to make good contact with the photoelectrode and counter electrode.

There are different types of polymer host matrix that have been used in quasi-solid state DSSCs such as poly(acrylonitrile-*co*-styrene), polyacrylonitrile (PAN), poly(vinyl pyridine-*co*-acrylic nitrile) and poly(acrylamide) (Lan et al. 2006; Ileperuma et al. 2011; Xiang et al. 2011; Wu et al. 2006). But till now, there is no report that has been published on DSSC employing polymer electrolyte with polyvinyl alcohol (PVA) as a host matrix. PVA is a synthetic polymer that possesses hydroxyl and carbonyl groups which enable it to interact with the ions from the salt. PVA is non-toxic, biocompatible, biodegradable, easy to prepare, chemically and thermally stable as well as exhibits excellent mechanical strength (Jia et al. 2007; Yang and Wu 2009). In this paper, we report on the preparation and characterization of PVA based quasi-solid state electrolytes and the performance of DSSCs employing such electrolytes. The cations in the electrolytes play a major role in improving the performance of DSSCs. The cations get adsorbed on the TiO<sub>2</sub> surface and strengthen the electronic coupling between the sensitizer and the surface (Kelly et al. 1999). According to Kelly et al. (1999), the adsorption of cations onto the surface of TiO<sub>2</sub> particles has a strong effect on the electron injection rate and the resulting quantum yield in DSSCs. They have studied iodide salts with different cations and inferred that the small cations show better adsorption to the TiO<sub>2</sub> surface. Using electrophoretic measurements, Pelet et al. (2000) also showed that cation adsorption increases when the size of the cation decreases. KI has shown to give good performance in DSSCs (Bandara et al. 2012) because of its relatively high charge density. Therefore we have chosen KI as the main iodide source in our electrolytes.

## 2 Experimental

### 2.1 Electrolyte preparation

First, a solution consisting of 0.1 g PVA, 0.4 g EC and 0.4 g PC dissolved in dimethyl sulfoxide (DMSO) was prepared. All chemicals used were obtained from Aldrich. Different amounts of KI (0.04, 0.06, 0.08 and 0.1 g) were then added to the solution. The solution was then heated to 393 K and maintained for 30 min until a viscous gel-like solution was formed. The gel was allowed to cool down to 323 K and some iodine crystals (10 % weight of salt) were added with continuous stirring until a homogenous gel polymer electrolyte was produced. Also a PVA gel polymer system containing two iodide salts of 9.9 wt% PVA, 39.6 wt% EC, 39.6 wt% PC, 6.5 wt% KI and 4.4 wt% C<sub>3</sub>H<sub>7</sub>NI (Pr<sub>4</sub>NI), was prepared using the same method. Iodine (10 % weight of salts) was also added to this system.

### 2.2 Electrochemical impedance spectroscopy

Electrochemical impedance spectroscopy (EIS) was used to determine the impedance of the electrolytes. The measurements were made using a Hioki 3531 Z Hitester in the frequency range 50 Hz to 1 MHz at different temperatures. The ionic conductivity,  $\sigma$  can be calculated from the equation given below:

$$\sigma = \frac{d}{R_b A} \quad (1)$$

In the equation,  $A$  and  $d$  are the area and thickness of the samples, respectively.  $R_b$  is the bulk resistance of the sample obtained from the complex impedance plot.

### 2.3 DSSC preparation

An indium tin-oxide (ITO) glass substrate was cleaned with distilled water and acetone. A thin compact TiO<sub>2</sub> layer was formed on the ITO glass with sheet resistance of 5  $\Omega$ /sq by spin coating 0.38 M diisopropoxytitanium bis(acetylacetonate) solution and then heat treated at 723 K for 30 min to act as a blocking layer for preventing back electron flow from the ITO into solar cell. TiO<sub>2</sub> paste (JGC Catalysts & Chemicals Ltd) was then doctor-bladed on the blocking layer. The area of active layer was 0.25 cm<sup>2</sup> and the thickness was 56  $\mu$ m. The TiO<sub>2</sub> layer was then sintered at 723 K for 30 min. After cooling down to 373 K, the TiO<sub>2</sub> electrode was immersed in *cis*-Ru(II) bis(2,2'-bipyridyl-4,4'-dicarboxylate)-(NCS)<sub>2</sub> red dye (or N3) solution for 24 h and the ITO sheet resistance is now 11  $\Omega$ /sq. The TiO<sub>2</sub> layer coated with dye was then washed with ethanol to remove any impurities. The TiO<sub>2</sub> photoelectrode was then immersed in 0.5 M 4-tert-butylpyridine (TBP) solution for 15 s in order to passivate the TiO<sub>2</sub>/dye interface. Platinum counter electrodes were prepared by brushing platinum solution (5 mmol L<sup>-1</sup> hexachloroplatinic acid solution in isopropanol) on top of an ITO glass and heat treated at 723 K for 30 min for the purpose to facilitate the transfer of charge between the electrode and redox couple. The DSSC was prepared by sandwiching the gel electrolyte between the dye coated electrode and platinum counter electrode.

### 2.4 Characterization

The photocurrent density–voltage ( $J$ – $V$ ) characteristics of the solar cells were obtained using the Keithley 2400 electrometer. The DSSCs were illuminated using a Xenon light source

of intensity of  $100 \text{ mW/cm}^2$ . The fill factor,  $ff$  and external light to electricity conversion efficiency,  $\eta$  were calculated using the following equations:

$$ff = \frac{V_{\max} \times J_{\max}}{V_{oc} \times J_{sc}} \quad (2)$$

$$\eta (\%) = \frac{V_{oc} \cdot J_{sc} \cdot ff}{P_{in}} \times 100 \% \quad (3)$$

Here  $J_{sc}$  is the short circuit current density,  $V_{oc}$  is the open circuit voltage,  $J_{\max}$  ( $\text{mA/cm}^2$ ) and  $V_{\max}$  (V) are the current density and voltage in the  $J$ - $V$  curves, respectively, at the point of maximum power output.  $P_{in}$  is the incident light power.

### 3 Results and discussion

#### 3.1 Ionic conductivity of electrolyte

Figure 1a shows the Nyquist plot of complex impedance for selected PVA gel polymer electrolytes. It can be observed that the Nyquist plot shows only the spike implying that electrode polarization is dominant in the frequency range used for the measurements. The

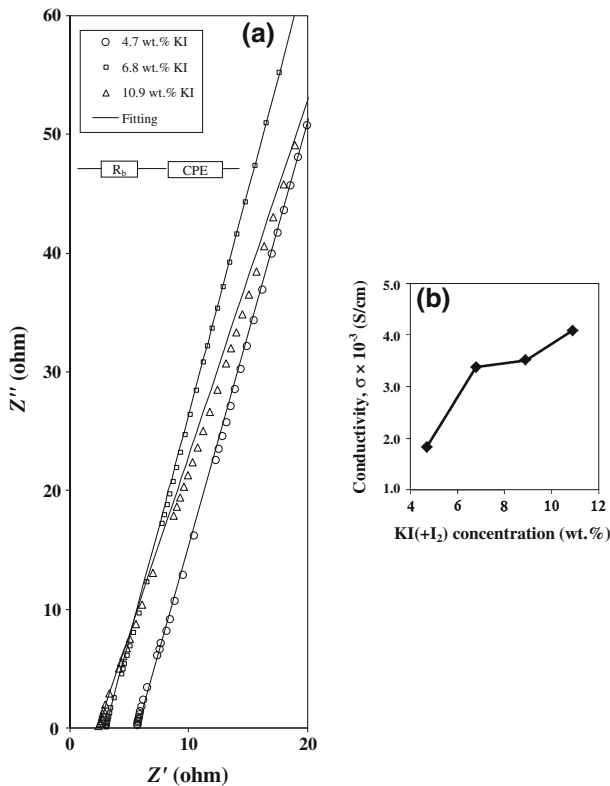


**Fig. 1** a Nyquist plot of complex impedance for PVA gel polymer electrolytes, b variation of ionic conductivity at room temperature with KI(+I<sub>2</sub>) concentration

impedance behavior can be described by an equivalent circuit comprising a resistor connected in series with a constant phase element, CPE as shown in Fig. 1a. The expressions for the real and imaginary parts of the impedance related to this equivalent circuit are given below:

$$Z' = R_b + \frac{\cos\left(\frac{\pi p}{2}\right)}{k^{-1}\omega^p} \tag{4}$$

$$Z'' = \frac{\sin\left(\frac{\pi p}{2}\right)}{k^{-1}\omega^p} \tag{5}$$

where  $Z'$  and  $Z''$  are the real and imaginary impedance parts, respectively.  $R_b$  is the bulk resistance of the samples and  $k^{-1}$  corresponds to the capacitance value of the CPE element,  $\omega$  is angular frequency ( $\omega = 2\pi f$  where  $f$  is frequency) and  $p$  a fraction of a right angle that the spike makes with the horizontal axis in the  $Z''$  versus  $Z'$  plot. As can be seen clearly in Fig. 1a, a good fit between the experimental data (represented as symbols) and the fitting line is obtained indicating that the equivalent circuit fits the experimental impedance data reasonably well. The parameters for the circuit elements obtained from the fitted lines are summarized in Table 1. From Table 1, it can be observed that as the KI concentration increases, the capacitance,  $k^{-1}$  and the conductivity increases.

Room temperature ionic conductivity for different salt concentrations is shown in Fig. 1b. It can be observed that the conductivity keeps on increasing with KI concentration and reaches  $4.1 \times 10^{-3}$  S/cm for the gel electrolyte with the composition of 9.9 wt% PVA: 39.6 wt% EC: 39.6 wt% PC: 10.9 wt% KI (+I<sub>2</sub>). The KI content was not increased further as the electrolyte system would become polymer in salt system. Ionic conductivity of electrolyte,  $\sigma$  depends on the charge carrier concentration,  $n$ , and carrier mobility,  $\mu$ , as described by the relation

$$\sigma = nq\mu \tag{6}$$

where  $q$  represent the charge on the mobile carrier. According to Eq. (6), increase in conductivity can be attributed to the increase in number density and or mobility of mobile ions or increase in the value of the product  $n\mu$  (Osman et al. 2001). In the gel polymer electrolyte system, solvation of salt by a solvent may form free ions, ion pairs and ion aggregates (Wu et al. 2006). The number of free ions and ion aggregates increase with increasing salt concentration and thereby giving rise to the observed initial increase in conductivity. The diffusion

**Table 1** Conductivity,  $k^{-1}$ ,  $p$ ,  $D$ ,  $\mu$ ,  $n$  for different electrolyte composition

| Electrolyte  | Conductivity (mS/cm) | $k^{-1}$ ( $\mu F$ ) | $p$ (radian) | $D$ ( $cm^2 s^{-1}$ ) | $\mu$ ( $cm^2 V^{-1} s$ ) | $n$ ( $cm^{-3}$ )     |
|--|----------------------|----------------------|--------------|-----------------------|---------------------------|-----------------------|
| 10.5 wt% PVA: 42.4 wt% EC: 42.4 wt% PC: 4.7 wt% KI(+I <sub>2</sub> ) | 1.83                 | 17.53                | 0.83         | $1.64 \times 10^{-6}$ | $6.28 \times 10^{-5}$     | $1.82 \times 10^{20}$ |
| 10.4 wt% PVA: 41.4 wt% EC: 41.4 wt% PC: 6.8 wt% KI(+I <sub>2</sub> ) | 3.38                 | 21.08                | 0.83         | $1.43 \times 10^{-6}$ | $5.46 \times 10^{-5}$     | $3.86 \times 10^{20}$ |
| 10.1 wt% PVA: 40.5 wt% EC: 40.5 wt% PC: 8.9 wt% KI(+I <sub>2</sub> ) | 3.57                 | 28.82                | 0.77         | $2.32 \times 10^{-6}$ | $8.88 \times 10^{-5}$     | $2.51 \times 10^{20}$ |
| 9.9 wt% PVA: 39.6 wt% EC: 39.6 wt% PC: 10.9 wt% KI(+I <sub>2</sub> ) | 4.08                 | 29.65                | 0.79         | $3.28 \times 10^{-6}$ | $1.26 \times 10^{-4}$     | $2.03 \times 10^{20}$ |

coefficient ( $D$ ), ionic mobility ( $\mu$ ) and charge carrier density ( $n$ ) can be calculated using the following equation (Bandara and Mellander 2011):

$$D = \frac{d^2}{\tau_2 \delta^2} \quad (7)$$

$$\mu = \frac{eD}{kT} \quad (8)$$

$$n = \frac{\sigma_{dc}}{e\mu} \quad (9)$$

Here,  $d = 1/2$  thickness of sample,  $\delta = d/\lambda$ ,  $\lambda = \varepsilon\varepsilon_0 A/k^{-1}$  is the electrical double layer thickness and  $\tau_2 = 1/\omega_2$  where  $\omega_2$  is the angular frequency at which the spike intersects the real impedance axis.  $\varepsilon_0$  is vacuum permittivity and  $\varepsilon$  is dielectric constant of gel polymer electrolyte. The values calculated for the parameters  $D$ ,  $\mu$ , and  $n$  using the values for electrical double layer capacitance  $k^{-1}$  obtained from the fittings of impedance data are summarized in Table 1. The electrical double layer thickness is the thickness of the ions that accumulate at the electrode/electrolyte interface. According to the results in Table 1, the number density and mobility of charge carriers vary for different salt concentrations. On increasing the wt. % of KI (+I<sub>2</sub>) up to 6.8 %, the number density of charge carriers has more than doubled and the mobility has reduced by 13%. The conductivity increased by about 85 % of the initial value of 1.83 mS/cm. The increase in number of ions is due to the increased amount of KI but the slight decrease in mobility may arise due to the electrostatic interaction between free ions. On further addition of KI salt [8.9 and 10.9 wt% KI (+I<sub>2</sub>)] the calculated number density of charge carriers has decreased and the ionic mobility has increased. However, the conductivity was observed to increase. The reduction in the number density may be due to formation of ion pairs and the increase in mobility of charge carriers may arise due to the lower electrostatic hindrance between the free ions which are relatively small in number due to the formation of neutral ion pairs which do not contribute to conductivity and do not affect mobility of the free ions. The increase of conductivity with more KI salt (>6.8 %) is due to increase in mobility of charge carriers which is dominant compared to the number density of charge carriers. Therefore, it can be inferred that the increase in conductivity with salt concentration can be attributed to the increase in either charge carrier density or mobility of mobile ions or both.

### 3.2 Solar cell

The operational principle of DSSC is illustrated in Fig. 2. The DSSC is consisting of (1) transparent conducting glass which allows natural sunlight to pass through to the active material, (2) dye molecules that can absorb incident light, (3) TiO<sub>2</sub> semiconductor which plays the important role in electron separation and transport process. The porosity of the TiO<sub>2</sub> layer determines the amount of dye molecules adsorbed on its surface. (4) The cathode made of a glass sheet coated with a catalyst (typically, platinum) to facilitate electron transfer and (5) an electrolyte containing a redox mediator. The charge separation in DSSC is based on electron transfer from dye molecule to TiO<sub>2</sub> and a hole transport from oxidized dye to electrolyte. The open circuit voltage is the difference between the Fermi level of TiO<sub>2</sub> and the redox potential of electrolyte. When exposed to sunlight, the electrons in the ground state of the dye absorb energy and occupy the excited state. Electrons in the excited state will then enter the conduction band of the semiconductor and travel to the counter electrode through the external circuit. In the meantime, redox mediator donates an electron to the dye

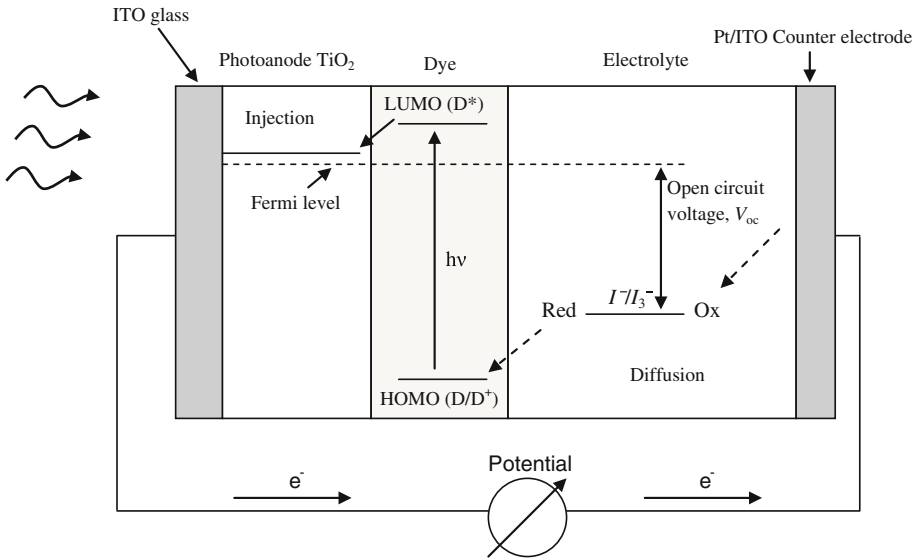
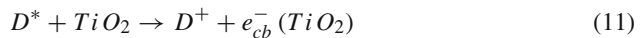


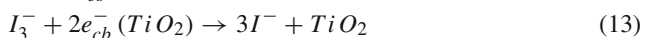
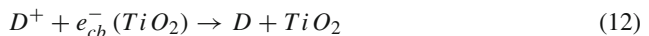
**Fig. 2** Schematic diagram of the DSSC structure and operating principle

and regenerates the dye and the mediator becomes oxidized. At the counter electrode, the oxidized form of redox mediator is reduced to its original state in the electrolyte. The cycle continues.

Figure 3 depicts the characteristics of photocurrent density versus voltage for DSSCs under the illumination of 100 mW/cm<sup>2</sup>. The values of  $J_{sc}$ ,  $V_{oc}$ ,  $ff$  and efficiency are listed in Table 2. The table also shows the variation in parameters for the cell (cell a) with electrolyte having 4.7 wt% KI in which the dye coated electrode is not treated with TBP. From Table 2, it can be seen that the values of  $V_{oc}$ ,  $ff$  and efficiency of DSSCs are increased when the TiO<sub>2</sub>/dye photoelectrode was treated by 4-tert-butylpyridine (TBP). This improvement of DSSC performance is due to the suppression of dark current at the electrode/electrolyte interface arising due to electron recombination (Lan et al. 2006). Under illumination ( $h\nu$ ), dye ( $D$ ) will be excited as in Eq. 10. The excited dye ( $D^*$ ) will inject an electron into the conduction band of TiO<sub>2</sub> and the excited dye will be oxidized ( $D^+$ ) (Eq. 11).



It is known that after the injection process, electrons in conduction band of TiO<sub>2</sub> will flow to the external circuit and completes the circuit or it can recombine with the oxidized dye (Eq. 12) or with  $I_3^-$  in the electrolyte (Eq. 13).



The recombination of electrons can result in the decrease of efficiency. To overcome this, the photoelectrode was treated with TBP which blocks the electron backflow and reduces recombination. The open circuit voltage of DSSC is dependent on the difference between redox potential in the electrolyte and Fermi level of TiO<sub>2</sub> electrode. TBP contains lone pair electrons at the nitrogen atom of pyridine ring. This lone electron pair is capable of interacting

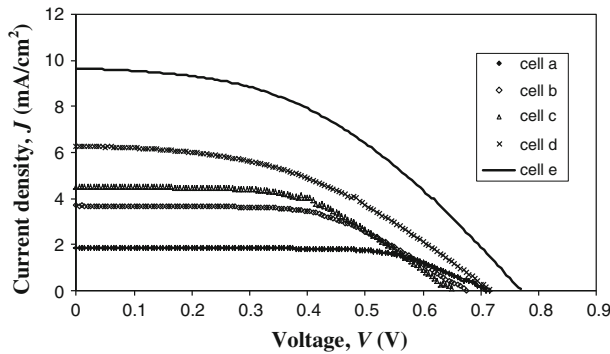


**Fig. 3**  $J$ - $V$  curve of DSSCs under illumination of  $100 \text{ mW/cm}^2$

**Table 2**  $J_{sc}$ ,  $V_{oc}$ ,  $ff$  and  $\eta$  of DSSCs using various compositions of electrolyte in gel form

| Cell | Electrolyte   | Conductivity (mS/cm) | $J_{sc}$ ( $\text{mA/cm}^2$ ) | $V_{oc}$ (V) | $ff$ | $\eta$ % |
|------|---|----------------------|-------------------------------|--------------|------|----------|
| a*   | 4.7 % KI (+I <sub>2</sub> )                           | 1.83                 | 2.31                          | 0.560        | 0.36 | 0.47     |
| a    | 4.7 % KI (+I <sub>2</sub> )                           |                      | 1.87                          | 0.715        | 0.66 | 0.88     |
| b    | 6.8 % KI (+I <sub>2</sub> )                           | 3.38                 | 3.69                          | 0.675        | 0.56 | 1.39     |
| c    | 8.9 % KI (+I <sub>2</sub> )                           | 3.57                 | 4.52                          | 0.655        | 0.54 | 1.60     |
| d    | 10.9 % KI (+I <sub>2</sub> )                          | 4.08                 | 6.27                          | 0.715        | 0.44 | 1.97     |
| e    | (6.5 % KI:4.4 % Pr <sub>4</sub> NI)(+I <sub>2</sub> ) | 2.18                 | 9.66                          | 0.770        | 0.44 | 3.27     |

a\* is a cell without TBP treatment on TiO<sub>2</sub>

with the Lewis acid group on TiO<sub>2</sub> surface thus shifting the Fermi level (Nazeeruddin et al. 1993; Cui et al. 2012). This leads to increase in  $V_{oc}$  and decrease in  $J_{sc}$ . According to literature (Kusama and Arakawa 2004a,b), the lone pair electrons at the nitrogen atom of alkyl amino pyridine also have some interactions with I<sub>2</sub> redox mediator resulting in the increment of  $V_{oc}$  and decrement of  $J_{sc}$ .

Table 2 lists the amount of salt in the electrolyte, short circuit current density, open circuit voltage, fill factor and efficiency of DSSCs fabricated with electrolytes having different salt concentrations. The cells a and a\* have the same electrolyte but in a\* the photoelectrode was not treated with TBP. Due to the presence of TBP, the cell a\* shows increased  $V_{oc}$  and decreased  $J_{sc}$  as expected. For the cells a–d with electrolytes having single iodide salt and TBP coating,  $J_{sc}$  and efficiency increase with increase in salt concentration. The improvement in solar cell performance with the increase of KI amount is attributed to the increase in the number and or mobility of redox mediators ( $I^-/I_3^-$ ). Redox mediator reactions at the electrolyte/electrode interfaces can be described as in the equations below;



The cell b has the electrolyte having 6.8 wt. % KI and therefore has more charge carriers compared to the cell a according to number density of charge carriers shown in Table 1. Hence the cell b has more  $I^-$  ions leading to more  $I^-/I_3^-$  redox couples and therefore has larger  $J_{sc}$ . On the other hand, the increase in  $J_{sc}$  for cells c and d can be attributed to increase



in mobility of redox couple as the number of charge carriers are less as shown in Table 1. The  $K^+$  cations in the electrolytes get adsorbed to the  $TiO_2$  surface easily because of their smaller size and lower the Fermi level and thereby assist the electron injection from dye to  $TiO_2$ . This enhanced injection also contributes to the higher currents observed in cells b–d. The lowering of Fermi level of  $TiO_2$  by  $K^+$  adsorption leads to lowering of  $V_{oc}$  in DSSCs and the amount of lowering depends on the number of  $K^+$  ions. This explains the observed lower  $V_{oc}$  values in cells c and b. In the cell d as the concentration of  $K^+$  is high the lowering of Fermi level of  $TiO_2$  can be large to facilitate higher injection rate so that the injected electrons may not have time to diffuse and therefore get collected at the  $TiO_2$ /electrolyte interface. Such accumulation of electrons will raise the Fermi Level and gives rise to higher open circuit voltage. This explains the relatively larger  $V_{oc} = 0.715$  V obtained for the cell d. The overall efficiency of a DSSC is determined by the combined effect of  $J_{sc}$ ,  $V_{oc}$  and  $\eta$  and in the present case the overall efficiency increases as the KI concentration in the electrolyte increases.

Table 2 also contains the parameters of a cell e with an electrolyte containing a binary iodide mixture of KI and  $Pr_4NI$ . The cell e with 9.9 wt% PVA-39.6 wt% EC-39.6 wt% PC-6.5 % KI-4.4 %  $Pr_4NI(+I_2)$  electrolyte exhibits the highest  $J_{sc}$ ,  $V_{oc}$  and  $\eta$ . In this electrolyte composition part of the KI in the electrolyte used in cell d has been replaced with  $Pr_4NI$  having large  $Pr_4N^+$  cations. In this electrolyte, as the bulky  $Pr_4N^+$  cation may not be very mobile and there may be more  $I^-$  ions originating from both iodide salts, the conductivity is expected to be dominated by  $I^-$  ions. From literature, it is known that DSSC employing electrolyte with binary salts improve the cell's efficiency (Bandara et al. 2012; Agarwala et al. 2011a,b). The ambient conductivity of the gel electrolyte used in cell e with double salts is  $2.18 \times 10^{-3}$  S/cm. From the results of DSSCs with gel polymer electrolyte containing only KI salt, it can be seen that  $J_{sc}$  increases with the conductivity of the electrolyte as in Table 2. But this is no longer valid in the case of cell e. The DSSC designated d which contains the electrolyte with highest conductivity of  $4.08 \times 10^{-3}$  S/cm than the electrolyte of cell e exhibits lower  $J_{sc}$ .  $Pr_4NI$  having big cation and low lattice energy can dissociate more efficiently compared to KI. This leads to higher iodide concentration in the electrolyte and thus increases  $J_{sc}$  in cell e. However, the low overall conductivity of electrolyte containing double salts is due to slow mobility of  $Pr_4N^+$  ions since it is a big cation. The higher  $V_{oc} = 0.770$  V in the cell e arises due to over all upward shift of Fermi level of  $TiO_2$  due to the combined effect of  $K^+$  cation adsorption and electron accumulation in  $TiO_2$ . The electrolyte contains  $K^+$  and  $Pr_4N^+$  cations. But mainly  $K^+$  get adsorbed to  $TiO_2$  surface as it is smaller compared to  $Pr_4N^+$ . Dissanayake and co-workers have reported that the efficiency of DSSC increase from 4.98 to 5.36 % using N719 dye and 10.4 wt% PAN, 41.4 wt% EC, 41.4 wt% PC, 1.1 wt% KI and 5.7 wt%  $Pr_4NI$  double salt gel electrolyte (Dissanayake et al. 2012).

Figure 4 depicts the characteristics of photocurrent density versus voltage for the dye-sensitized solar cell (cell e) containing the binary salt electrolyte under different intensity of illumination. Table 3 gives the  $J_{sc}$ ,  $V_{oc}$  and  $\eta$  for the cell under illumination of different intensities and Fig. 5 shows the variation of these parameters with intensity of light. It can be observed that both  $J_{sc}$  and  $V_{oc}$  increase with the increase in intensity. It is interesting to note that highest efficiency of 4.59 % is obtained at the low intensity of  $54.1$  mW/cm<sup>2</sup>. Wang et al. (2003) have also reported higher efficiency at lower intensity with efficiency changing from 6.1 % under 1 Sun ( $100$  mW/cm<sup>2</sup>) to 7.6 % at 0.01 Sun. As mentioned previously, after injection of electron from excited state of dye into conduction band of  $TiO_2$ , some electrons will flow to the external circuit and some will recombine at the  $TiO_2$ /electrolyte interface. Increasing light intensity results in higher electron density in the  $TiO_2$  film giving rise to

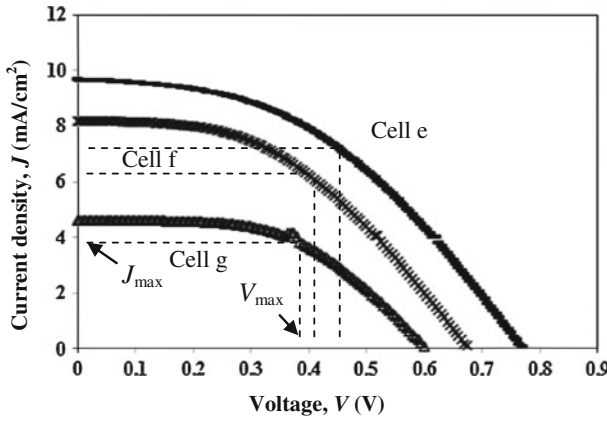


**Fig. 4**  $J$ - $V$  curve of DSSCs under different intensities of light

**Table 3**  $J_{sc}$ ,  $V_{oc}$ ,  $ff$  and  $\eta$  of DSSCs under different intensities of light

| Cell | Intensity (mW/cm <sup>2</sup> ) | $J_{sc}$ (mA/cm <sup>2</sup> ) | $V_{oc}$ (V) | $P_{max}$ (mW/cm <sup>2</sup> ) | $ff$ | $\eta$ % |
|------|---------------------------------|--------------------------------|--------------|---------------------------------|------|----------|
| e    | 100                             | 9.66                           | 0.770        | 3.26                            | 0.44 | 3.27     |
| f    | 54.1                            | 8.18                           | 0.675        | 2.49                            | 0.45 | 4.59     |
| g    | 36.1                            | 4.61                           | 0.600        | 1.54                            | 0.56 | 4.29     |

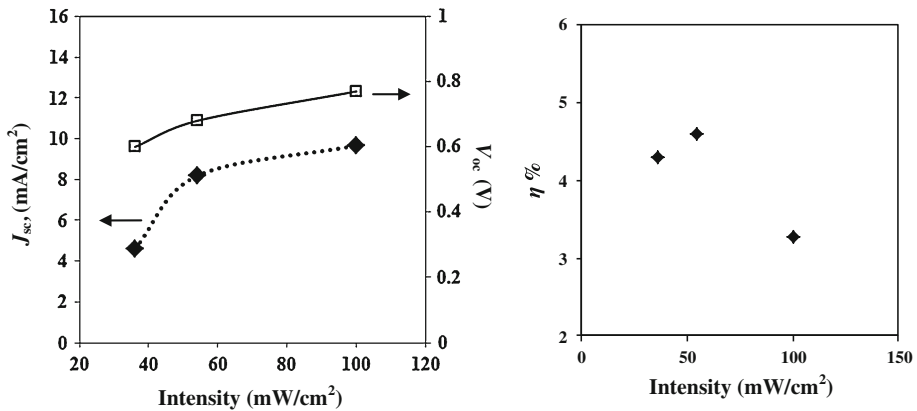


**Fig. 5**  $J_{sc}$ ,  $V_{oc}$ ,  $ff$  and  $\eta$  of DSSCs under different light of intensity

higher  $J_{sc}$  and accumulated electrons due to slow diffusion in  $TiO_2$  shifts the Fermi level of  $TiO_2$  upwards so that the  $V_{oc}$  is higher. At the same time higher electron density leads to increase in the recombination rate at the  $TiO_2$ /electrolyte interface resulting in lower effective  $J_{sc}$  and hence lower overall efficiency (Lee et al. 2009). Very low intensity light gives lower current density and lower  $V_{oc}$  and therefore results in much lower overall power conversion efficiency.

## 4 Conclusions

Dye sensitized solar cells with electrolytes containing PVA as polymer host, KI and Pr<sub>4</sub>Ni as salts have been successfully fabricated. The overall power conversion efficiency of DSSCs with electrolyte having KI salt alone increases with KI concentration. The DSSC with electrolyte having 10.9 wt % KI shows the best power conversion efficiency of 1.97 % under illumination of 100 mW/cm<sup>2</sup>. However, the short circuit current density  $J_{sc}$  depends on the iodide ion conductivity of the electrolyte which controls the redox activity and the cations present in the electrolyte controls both electron injection and open circuit voltage  $V_{oc}$ . The efficiency of the best DSSC improved further to 3.27 % when part of the KI in the electrolyte was replaced with larger Pr<sub>4</sub>Ni salt. This can be attributed to the increase in  $J_{sc}$  due to better electron injection facilitated by better adsorption of smaller K<sup>+</sup> cations onto TiO<sub>2</sub> surface and higher iodide conductivity promoted by the presence of larger Pr<sub>4</sub>N<sup>+</sup> cations. Under low light intensity of 54.1 mW/cm<sup>2</sup>, the DSSC with the double salt electrolyte exhibits a better efficiency of 4.59 %. This is due to low recombination rate of electrons facilitated by low rate of excitation under low light condition.

**Acknowledgments** The Authors thank University of Malaya for the AFR Program grant No. RP003D-13AFR.

## References

- Agarwala, S., Thummalakunta, L.N.S.A., Cook, C.A., Peh, C.K.N., Wong, A.S.W., Ke, L., Ho, G.W.: Co-existence of LiI and KI in filler-free, quasi-solid-state electrolyte for efficient and stable dye-sensitized solar cell. *J. Power Sourc.* **196**, 1651–1656 (2011a)
- Agarwala, S., Peh, C.K.N., Ho, G.W.: Highly stable quasi-solid state dye sensitized solar cell: improved performance using diphenylamine in filler free KI and LiI electrolyte. *Appl. Mater. Interface* **3**, 2383–2391 (2011b)
- Bandara, T.M.W.J., Mellander, B.-E.: Evaluation of mobility, diffusion coefficient and density of charge carriers in ionic liquids and novel electrolytes based on a new model for dielectric response. In: Kokorin, Alexander (ed.) *Ionic Liquids: Theory, Properties, New Approaches*, pp. 383–406. InTech Janeza Trdine, Croatia (2011)
- Bandara, T.M.W.J., Dissanayake, M.A.K.L., Jayasundara, W.J.M.J.S.R., Albinsson, I., Mellander, B.-E.: Efficiency enhancement in dye sensitized solar cells using gel polymer electrolytes based on a tetrahexylammonium iodide and MgI<sub>2</sub> binary iodide system. *Phys. Chem. Chem. Phys.* **14**, 8620–8627 (2012)
- Chiba, Y., Islam, A., Watanabe, Y., Komiya, R., Koide, N., Han, L.: Dye-sensitized solar cells with conversion efficiency of 11.1%. *Jpn. J. Appl. Phys.* **45**, L638–L640 (2006)
- Cui, Y., Zhang, J., Zhang, X., Feng, J., Hong, Y., Zhu, Y.: High performance quasi-solid-state dye-sensitized solar cells based on acetamide-modified polymer electrolytes. *Org. Electron.* **13**, 2561–2567 (2012)
- Dissanayake, M.A.K.L., Thotawatthage, C.A., Senadeera, Bandara, T.M.W.J., Jayasundera, W.J.M.J.S.R., Mellander, B.-E.J.: Efficiency enhancement by mixed cation effect in dye-sensitized solar cells with PAN based gel polymer electrolyte. *Photochem. Photobiol. A Chem.* **246**, 29–35 (2012)
- Grätzel, M.: Dye-sensitized solar cells. *J. Photochem. Photobiol. C Photochem. Rev.* **4**, 145–153 (2003)
- Ileperuma, O.A., Kumara, G.R.A., Yang, H.-S., Murakami, K.: Quasi-solid electrolyte based on polyacrylonitrile for dye-sensitized solar cells. *J. Photochem. Photobiol. A Chem.* **217**, 308–312 (2011)
- Jeonga, W.-S., Lee, J.-W., Jung, S., Yun, J.H., Parka, N.-G.: Evaluation of external quantum efficiency of a 12.35% tandem solar cell comprising dye-sensitized and CIGS solar cells. *Solar Energy Mater. Solar Cell.* **95**, 3419–3423 (2011)
- Jia, Y.-T., Gong, J., Gu, X.-H., Kim, H.-Y., Dong, J., Shen, X.-Y.: Fabrication and characterization of poly(vinyl alcohol)/chitosan blend nanofibers produced by electrospinning method. *Carbohydr. Polym.* **67**, 403–409 (2007)
- Kelly, C.A., Farzad, F., Thompson, D.W., Stipkala, J.M., Meyer, G.J.: Cation controlled interfacial charge separation in sensitized nanocrystalline TiO<sub>2</sub> photoanodes. *Langmuir* **15**, 7047–7054 (1999)

- Kusama, H., Arakawa, H.: Influence of alkylaminopyridine additives in electrolytes on dye-sensitized solar cell performance. *Sol. Energy Mater. Sol. Cells*. **81**, 87–99 (2004a)
- Kusama, H., Arakawa, H.: Influence of aminotriazole additives in electrolytic solution on dye-sensitized solar cell performance. *J. Photochem. Photobiol. A Chem.* **164**, 103–110 (2004b)
- Lan, Z., Wu, J., Wang, D., Hao, S., Lin, J., Huang, Y.: Quasi-solid state dye-sensitized solar cells based on gel polymer electrolyte with poly(acrylonitrile-co-styrene)/NaI/I<sub>2</sub> sol. *Solar Energy* **80**, 1483–1488 (2006)
- Lan, Z., Wu, J., Lin, J., Huang, M., Li, P., Li, Q.: Influence of ionic additives NaI/I<sub>2</sub> on the properties of polymer gel electrolyte and performance of quasi-solid-state dye-sensitized solar cells. *Electrochim. Acta* **53**, 2296–2301 (2008)
- Lee, K.-M., Wu, S.-J., Chen, C.-Y., Wu, C.-G., Ikegami, M., Miyoshi, K., Miyasaka, T., Ho, K.-C.: Efficient and stable plastic dye-sensitized solar cells based on a high light-harvesting ruthenium sensitizer. *J. Mater. Chem.* **19**, 5009–5015 (2009)
- Nazeeruddin, M.K., Kay, A., Rodicio, I., Humphry-Baker, R., Muller, E., Liska, P., Vlachopoulos, N., Grätzel, M.: Conversion of light to electricity by cis-X<sub>2</sub>Bis(2,2'-bipyridyl-4,4'-dicarboxylate)ruthenium(II) charge-transfer sensitizers (X = Cl-, Br-, I-, CN-, and SCN-) on nanocrystalline TiO<sub>2</sub> electrodes. *J. Am. Chem. Soc.* **115**, 6382–6390 (1993)
- Nazeeruddin, M.K., Pechy, P., Grätzel, M.: Engineering of efficient panchromatic sensitizers for nanocrystalline TiO<sub>2</sub>-based solar cells. *J. Am. Chem. Soc.* **123**, 1613–1624 (2001)
- O' Regan, B., Grätzel, M.: A low-cost, high-efficiency solar cell based on dye-sensitized colloidal TiO<sub>2</sub> films. *Nature* **353**, 737–740 (1991)
- Oskam, G., Bergeron, B.V., Meyer, G.J., Searson, P.C.: Pseudohalogens for dye-sensitized TiO<sub>2</sub> photoelectrochemical cells. *J. Phys. Chem. B* **105**, 6867–6873 (2001)
- Osman, Z., Ibrahim, Z.A., Arof, A.K.: Conductivity enhancement due to ion dissociation in plasticized chitosan based polymer electrolytes. *Carbohydr. Polym.* **44**, 167–173 (2001)
- Pelet, S., Moser, J.E., Gratzel, M.: Cooperative effect of adsorbed cations and iodide on the interception of back electron transfer in the dye sensitization of nanocrystalline TiO<sub>2</sub>. *J. Phys. Chem. B* **104**, 1791–1795 (2000)
- Santa-Nokki, H., Busi, S., Kallioinen, J., Lahtinen, M., Korppi-Tommola, J.: Quaternary ammonium polyiodides as ionic liquid/soft solid electrolytes in dye-sensitized solar cells. *J. Photochem. Photobiol. A Chem.* **186**, 29–33 (2007)
- Sapp, S.A., Elliott, C.M., Contado, C., Caramori, S., Bignozzi, C.A.: Substituted polypyridine complexes of cobalt(II/III) as efficient electron-transfer mediators in dye-sensitized solar cells. *J. Am. Chem. Soc.* **37**, 11215–11222 (2002)
- Wang, P., Zakeeruddin, M.Z., Moser, J.E., Nazeeruddin, M.K., Sekiguchi, T., Gratzel, M.: A stable quasi-solid-state dye-sensitized solar cell with an amphiphilic ruthenium sensitizer and polymer gel electrolyte. *Nat. Mater.* **2**, 402–407 (2003)
- Wu, J., Lan, Z., Wang, D., Hao, S., Lin, J., Wei, Y., Yin, S., Sato, T.: Quasi-solid state dye-sensitized solar cells-based gel polymer electrolytes with poly(acrylamide)–poly(ethylene glycol) composite. *J. Photochem. Photobiol. A Chem.* **181**, 333–337 (2006)
- Wu, J., Lan, Z., Wang, D., Hao, S., Lin, J., Huang, Y., Yin, S., Sato, T.: Gel polymer electrolyte based on poly(acrylonitrile-co-styrene) and a novel organic iodide salt for quasi-solid state dye-sensitized solar cell. *Electrochim. Acta* **51**, 4243–4249 (2006)
- Xiang, W., Fang, Y., Lin, Y., Fang, S.: Polymer-metal complex as gel electrolyte for quasi-solid-state dye-sensitized solar cells. *Electrochim. Acta* **56**, 1605–1610 (2011)
- Yang, C.-C., Wu, G.M.: Study of microporous PVA/PVC composite polymer membrane and its application to MnO<sub>2</sub> capacitors. *Mater. Chem. Phys.* **114**, 948–955 (2009)